Proceedings World Geothermal Congress 2020+1
Reykjavik, Iceland, April - October 2021

Geological, Hydrogeological and Geophysical Survey of the Xumai Geothermal Field in Tibet, China

ZHANG Song[1], Xie Yingchun[2], CHENG Jixing[1], HAO Weilin[1], WAN Hanping[1], LIU Hongxu[1], HAN Jun[1]

1. Beijing Research Institute of Uranium Geology

10 Anwai Xiaoguan Dongli, Chaoyang District, Beijing, China

2. CNNP Kunhua Energy Development Co.,Ltd.

Wangjun International,1359 Gudun Road,Yuhang District,Hangzhou,China

Zhangsong1891@163.com

Keywords: Xumai geothermal field, Geothermal resources exploration, Hydrogeological and geophysical survey, Tibet

ABSTRACT

Xumai geothermal field locates in the southern of Naqu-Nimu geothermal belt, which is the most important geothermal belt in Tibet, even in the whole country. There are lots geothermal fields in the belt, including the famous Yangbajing geothermal field. In order to evaluate the geothermal resources for further exploration, geological, hydrogeological and geophysical survey were carried out in the Xumai geothermal field. The thermal activities are still present on the surface with the highest temperature of 76°C. The geological works show that four group fractures exist in this area, and the strikes are SN, EW, NE and NW. Among them, the SN-striking fracture F1 is considered to control the thermal activities due to the fact that most hot spring spots occur along this fracture The hydrogeological work shows that the hydrochemical type is HCO_3-Na in the northern wihle SO_4·Cl·HCO_3-Na in the southern of the Xumai geothermal field. The source of the hot spring water is proved to be atmospheric precipitation by the hydrogen and oxygen isotopes. The highest temperature of the geothermal reservoir is 164.4°C, which is calculated by the SiO_2 geothermometer. Geophysics works, including magnetotelluric (MT), Audiomagnetotelluric (AMT) and gravity surveys were also carried out in this area. The fracture F1 and its secondary fractures can be identified clearly by banded low resistivity anomaly. Based on the above works, we can conclude that: 1) the reservoir is zonal, controlling by the F1 and its secondary fractures. 2) The surrounding rocks of the reservoir are granite and granodiorite, and no obvious cap was recognized. 3) The Xumai geothermal field is a good candidate for the exploitation of geothermal resource, and drilling works are suggested to validate deep geothermal resources.

1. INTRODUCTION

Tibet possesses abundant geothermal resources due to its specific geological setting. There are four important geothermal belts with strike of SN in Tibet. They are Nimu–Nagchu geothermal belts, Shenzha-Dingjie geothermal belts, Nima-Dingri geothermal belts and Longger geothermal belts. The Nimu–Nagchu geothermal belt is the most important for their abundant geothermal resources. Some famous geothermal fields are located in this belt, such as Yangbajing, Yangyi, and Gulu geothermal field (Duo et al., 2003; Liu et al., 2014).

The origin of the geothermal fluids, distribution of heat sources, genesis of geothermal fields and the conceptual model of the geothermal field in Tibet were investigated carefully, especially in the Yangbajing and Yangyi geothermal field. (Duo et al., 2003; Zhao et al., 1998, 2002; Pang et al., 1998; Guo et al.,2007; Yuan et al., 2014). However, there are lots of other geothermal fields in the Nimu–Nagchu geothermal belt, such as Xumai geothermal field, Gulu geothermal field, Ningzhong geothermal field, Yuzhai geothermal field, and so on. Compared with their abundant geothermal resources, the research and exploration works are limited. The geology, hydrogeology, genesis, and the resource potential are not clear. If we want to make good use of these geothermal resources, lots of works need to be done.

Xumai geothermal field, locate in the south of the Nimu–Nagchu geothermal belt, is about 115 km in the west of Lhasa city, Tibet, western China. There are several thermal anomaly areas in Xumai, and the temperature of the hot springs can reach to 80 degrees in the surface. Some people thought that electricity generation is feasible in the Xumai geothermal field. In the process of this study, the geological, hydrogeological and geophysical conditions in Xumai geothermal field were analyzed carefully to find out the good perspective area.

2. GEOLOGY

2.1 Rock types

The Xumai geothermal field is located in an NS-striking intermontane half-graben (Xumai Basin). The deposits in the basin consist of mainly Quaternary slope deposit and locally tillite and alluvium. The granodiorite and biotite adamellite formed from late Yanshanian to early Himalayan are distributed around this basin (Fig. 1).

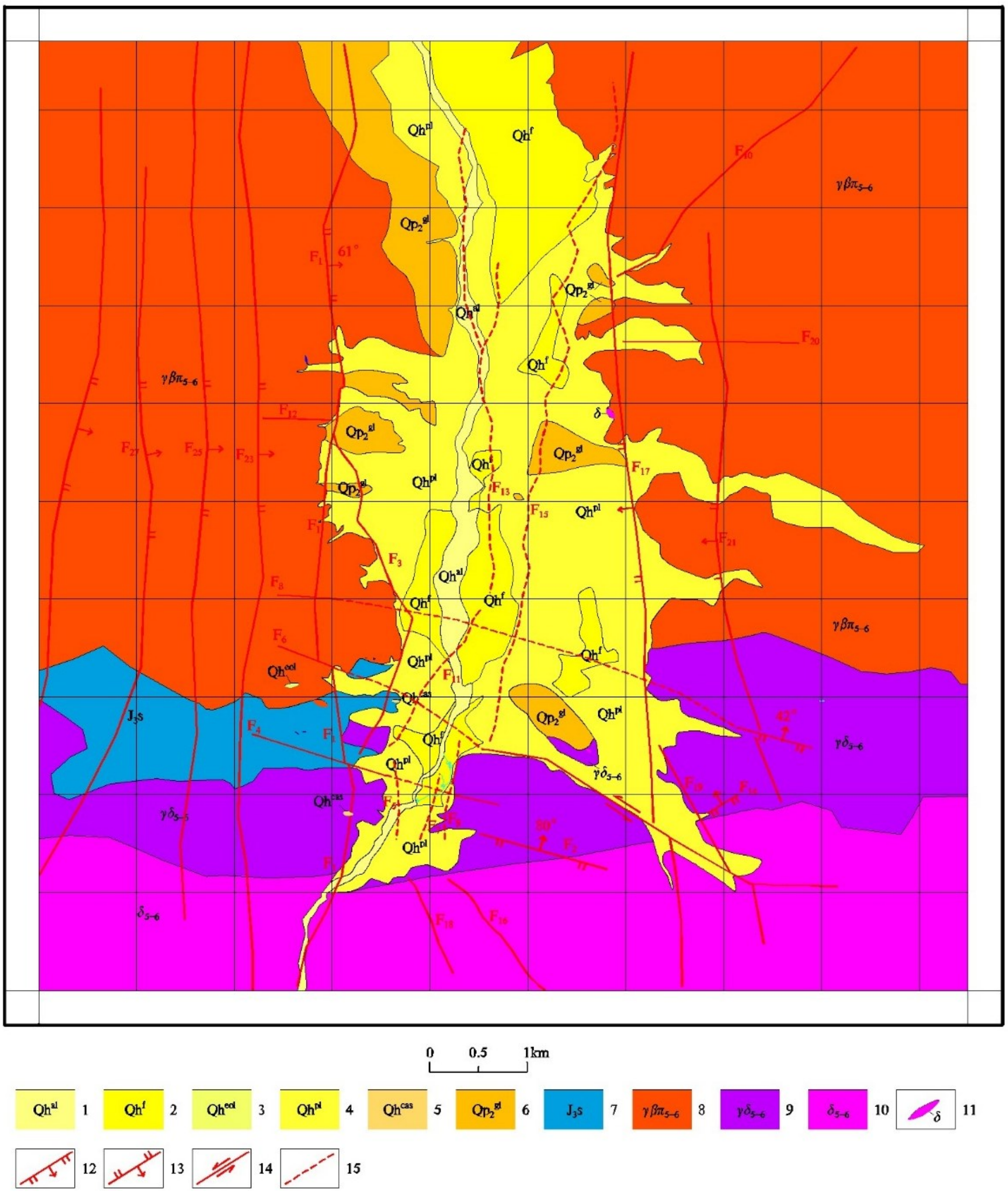

Figure 1: The geological sketch map of the Xumai area

1-alluviation; 2-marsh; 3-eluvium; 4-proluvial; 5-sinter; 6-glacial drift; 7-slate; 8-porphyritic monzonitic granite; 9-granodiorite; 10-diorite; 11-dykes; 12-normal fault; 13- reverse fault; 14- strike-slip fault; 15-inferred fault

The strata are mainly Upper Jurassic Sangriqun Formation ($J_{3}sr$), Quaternary Middle Pleistocene moraine (Qp_2^{gl}), Holocene slope diluvial gravel (Qh^{spl}), alluvial gravel (Qh^{al}) and swamp accumulation (Qh^{f}).

The magmatic rocks in the Xumai geothermal field mainly consist of coarse-grained porphyritic biotite monzonite, granodiorite, and diorite.

The coarse-grained porphyritic biotite monzonite distributes on the mountains to the north of the Xumai, more than 10 km^2 in area. They are white in color, porphyritic-like texture, and massive structure. The rock is composed of potassium feldspar (40%), plagioclase (30%), quartz (25%), and biotite (5%). The Phenocrysts are mainly potassium feldspar crystal, following the quartz crystal.

The fine granodiorite is grey in color, fine-grained granitic texture, and massive structure. The rock is composed of plagioclase (40%), quartz (35%), potassium feldspar (10%), and hornblende (5%). Clay alternation has been occurred in these rocks along the F1 in the western margin of the basin, forming an alteration zone with width about 100–150 m.

The diorites are distributed in the southern of the work area. The rock is composed of plagioclase (50%), hornblende (30%), potassium feldspar (10%) and biotite (5%).

2.2 Structure

The structures in the basin are mainly brittle, and they could be divided into four groups according to the different trends: the nearly NS-, nearly EW-, NE- and NW-striking structures. The NS-striking structures are most developed and control the formation and development of the Xumai Basin. These faults were formed accompanying with the famous Yadong-Gulu rift belt. More than five relative large scale faults have been recognized in the western margin of the basin.

The basin-controlling faults F1 and F23 are first-order structures, which have intimate relationship with the geothermal reservoir in the deep. They are 100–400 m wide and more than 5 km long, respectively. Here we present some main faults relating with the geothermal resources.

F1 is the most important fault in the western margin of the basin, with a width >500 m. It is a segment of the Jiuzila-Dangxiong-Yangbajing-Nimu Fault. It has been considered to be a multiphase active East-dipping (55~65°) normal fault. Fault gouges and facet can be recognized. The fault F7 is exposed in the southern of the basin, and covered by the Quaternary deposits in the interior. It is a nearly upright NNE-striking normal fault, with attitudes of 300°∠88° to the south of the F4, and 95°∠75° to the north. This fault could be divided into strong and weak deformation zones depending on the deformation degree. Fault gouges, cataclastic rocks, and fault facets are developed in the strong deformation zones; and only concentrated joint bands are found in the weak deformation zones. F9 is a nearly NS-striking transtension fracture, with an East-dipping of 75°. Its width in the southern part is about 50 m, and change narrow in the northern part. Similar to F7, the F9 also could be divided into strong and weak deformation zones.

The WE-striking fracture F2 is about 30 m in the width, and its attitude is 15°∠80°. Its secondary structures have been observed, and usually they are N- or S-dipping. Quartz diorite and some mafic dykes were involved in the fracture zone, and a lot of tectonite can be recognized, including tectonic lens, protocataclasite, cataclasite, and fault gouge. Some fracture structural elements, such as drag folds, conjugate share joints, and striae, suggest that F2 is a dextral strik-slip thrust fault (Fig. 2).

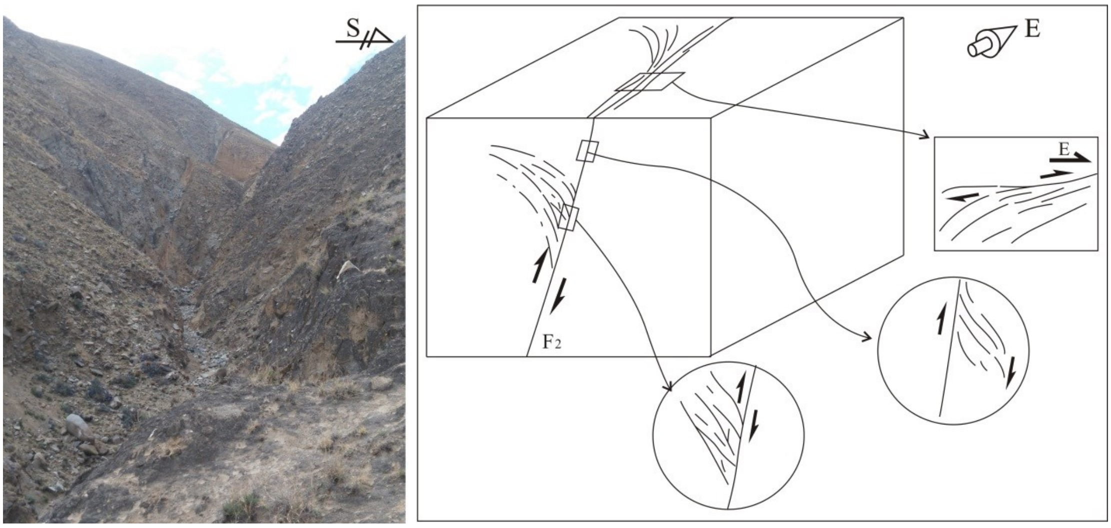

Figure 2: The structural characteristic of the F2

3.3 Alteration Characteristics

Clay alteration is one of the most obvious and representative alteration types in this area, which provides the evidence for the paleogeothermal activities. Clay-altered rocks are mainly coarse-grained porphyritic biotite monzonite. Since the clay minerals, such as kaolinite, were formed during the alteration, the rocks turned to be white color and the hardness was obviously reduced. In some strong altered places, the rocks presented to be white powders. The alteration area shows characteristics of zonal distribution, usually along the fractures. The alteration is relatively strong on both sides of the fractures, and decreases rapidly away from the fractures, reflecting that the alteration temperature of water and steam was not high enough to influence a larger range. Besides the clay alteration, epidotization, chloritization, silication and carbonization have been observed in the area.

3.4 Distribution of the Geothermal Anomaly Areas

Four geothermal anomaly areas were recoginzed in the Xumai Basin. They are Jiba village, Southern Xumai village, Western Xumai village and Angang village geothermal anomaly areas. Among them, the Jiba village geothermal anomaly area is out of our study area. The anomaly in the Angang village and Western Xumai village is weakly. The Angang village anomaly distributes as a belt about 200m in the length along the F1. The geothermal anomaly in Southern Xumai village is strong and has a relative larger range: a belt along the Reshui and Xuqu rivers.

3. HYDROGEOLOGICAL CHARACTERISTICS

3.1 Hydrogeological Conditions

The groundwater types in the work area are divided into fracture aquifer of base rocks and pore aquifer of loose rocks, according to the topography, lithology, groundwater burial conditions, aquifer medium, hydraulic characteristics, and natural storage conditions of groundwater. Fracture aquifer of bedrock is mainly distributed in the surrounding mountainous areas of the work area, and its lithology is mainly Cretaceous coarse-grained porphyry granite, fine-grained granite, granite diorite, and diorite. The fracture structures are very developed in the work area. The fragmentized rocks near the fractures provide a good permeability, forming water-rich zones along the fractures. Pore aquifer of loose rocks consists of Quaternary slope, diluvial, moraine, and alluvial deposits.

Swamp accumulation explores locally. These loose rocks mainly distribute in the margin and interior of the basin, presenting as farmland, woodland, swamp, and so on.

3.2 hydrogeochemistry

The pH of Xumai water samples was ranging between 7.44 and 8.38, which belongs to neutral to weak alkaline water. Among the water samples, the pH of hot spring water has a higher average pH of 8.30, slightly lower than 8.81–9.04 in Yangbajing-Gulu area. According to the hydrochemical data of water samples, the cations are Na^+, K^+, Ca^{2+}, Mg^{2+}, and the anions are HCO_3^-, Cl^-, SO_4^{2-}. In the most water samples of cold springs, rainwater and surface water, the mainly content of cation is $Ca^{2+} > Na^+$ and $K^+ > Mg^{2+}$; and the content of anions is $HCO_3^- > SO_4^{2-} > Cl^-$. The ion contents of hot spring and borehole hot water samples are dominated by Na^+ and K^+, followed by Ca^{2+} and Mg^{2+}. $SO_4^{2-}$and Cl^- were the main anions in hot spring water samples from Xumai, Yangyi, and Yangbajing areas, while the content of HCO_3^- was the highest anion in Gulu area.

Piper diagram can be used to analyze the hydrochemical types of water samples, not only for the classification of hydrochemistry, but also for analysis of groundwater evolution, such as cation exchange. The water chemical composition of cold springs, surface water, snow water, and rainwater in this area mainly distributes in the areas dominated by Ca^{2+} and HCO_3^-, while that of hot springs and boreholes is dominated by Na^+ where is marked by the red line (Fig.3).

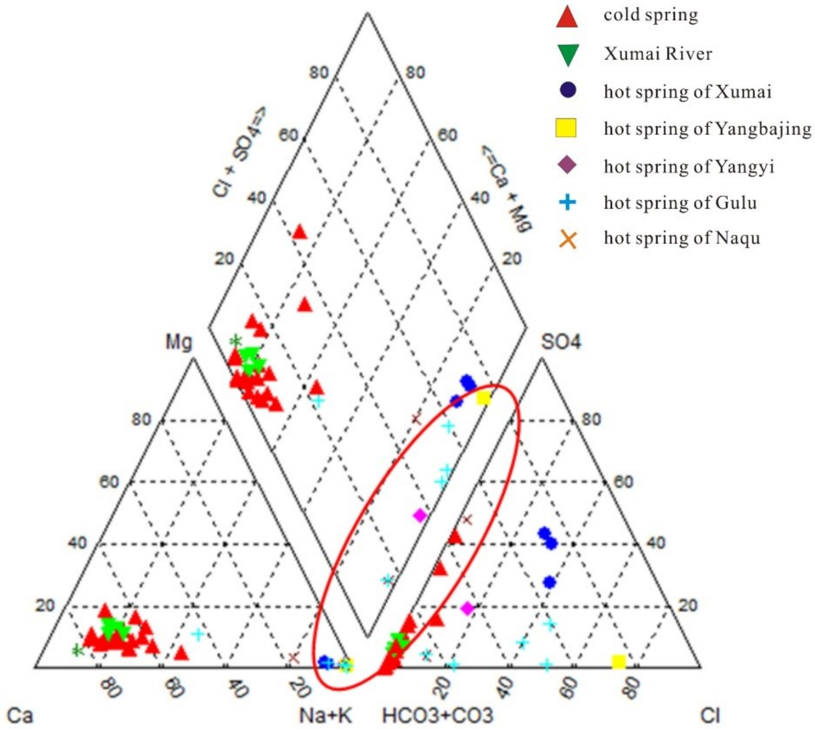

Figure 3: The Piper map of the water sample in Tibet

The TDS content of hot spring water in the Xumai area is about 500 mg/L, while that of hot spring water and borehole hot water in the Yangbajing-Guluarea is about 1 g/L–3.7 g/L. This indicates that the cyclic alternation of hot spring water in the Xumai is relatively slow, far lower than the rate of water renewal of atmospheric precipitation and surface water, but higher than that of hot spring and borehole hot water in the Yangbajing-Gulu area. This is mainly due to the strong recharge and mixing of shallow groundwater and surface water in the hot spring groundwater in the Xumai area.

4. GEOPHYSICAL SURVEY

4.1 Magnetotelluric Analyses

Four magnetotelluric sections have been analyzed. The distance of the measurement points was usually 100 m, while turned it to be 200 m in some places due to the steep landform (Fig.4).

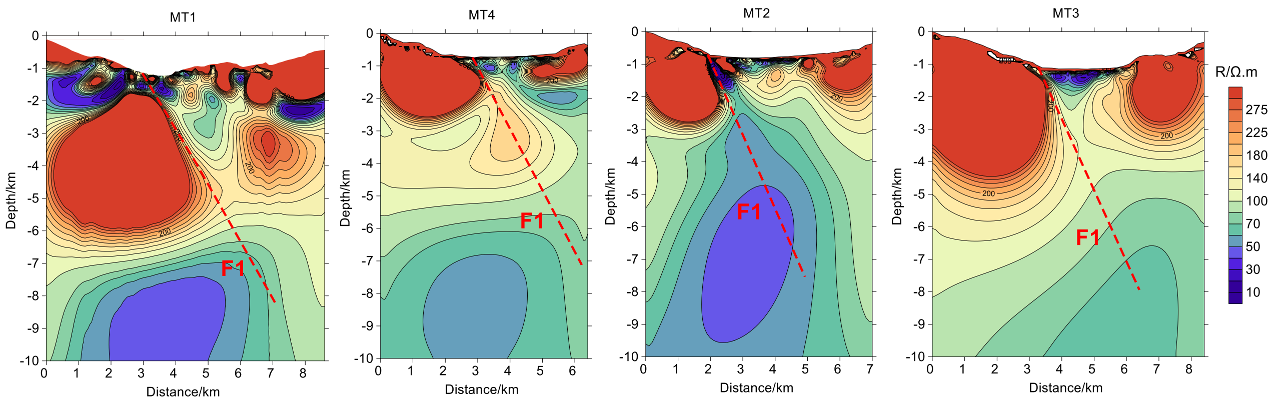

Figure 4: the two-dimensional inversion cross section map of MT

The inversion results of the section MT1 suggest the granite pluton is about 6–7 km in the thickness; the shallow low resistance body, corresponding to the range of 3–4 km on the section, was considered to be the responses to the thermal reservoir of the springs in the southern of the Xumai geothermal field. The AMT sections L2 and L4 yielded the consistent inversion results with the section MT1; two low resistance bodies existed in a shallow depth under the range 1–3 km of the section, which were inferred to be two NS-striking and W-dipping normal faults. In this section, the dip angle of F1 is about 60 °.

According to the inversion results of section MT4, the thickness of the granite pluton is about 5–6 km. A low resistance body has been recognized under the range 2–5 km of the section, indicating the existence of the Quaternary aquifer. The angle of F1 is about 50 ° in this section.

The inversion results of the section MT2 reveal the lower resistance body underground is larger in the scale, shallower in the depth, and lower in the resistance. The fault F1 cut near to the earth surface, with a dip angle of 60 °. There is an obvious low resistance body under 2 km of the section, corresponding to the strongest alternation area on the earth surface, where is the location of the Angang Spring.

The granite pluton is 5–7 km in the thickness depending on the inversion results of the section MT3. The dip angle of F1 is about 60 °. A large-scale low resistance body is under the range of 3–6 km of the section, representing a large-scale Quaternary aquifer, with a max thickness > 1 km.

Based on the inversion results of the MT sections, it is conclude that the electrical structures yielded by all the sections are consistent, indicating the characteristics that: 1) the low resistance bodies are revealed. Combined with the electrical structures and heat storage model of Yangbajing, the low resistance bodies are speculated to be deep melts, which play the role of the thermal sources for the Xumai geothermal field. 2) A low resistance belt has been recognized in the granite pluton, which is regarded as the reflex of the basin-controlling fault F1 and its fracture zone. The fault F1 and its fractures connect with the geothermal source in the deep, providing a heat channel for the Xumai geothermal field.

4.2 Automagnetotelluric analyses

There are 32 WE-directing sections have been performed in the study area, the distance between analysis points is 25 m. The reflected electrical structures by adjacent sections have a good correlation and reveal the stratigraphic structure and the distribution of the fault structures.

(1) L2 AMT section

Except for the low resistance body mentioned above, electrical differences under the ranges of 960–1000m and 1360–1480 m have been recognized in the section L2, which interpreted as two second-order faults in the base rocks: one is E-dipping fault, and the other is W-dipping (Fig.5).

It is inferred that the Quaternary is about 50 m in depth based on the low resistance under the range 0–520 m of the section L2. Since the low resistance anomaly maybe caused by the fractures of the base rocks, it needs further works to verify if the lower boundary of the anomaly is the upper boundary of the base rocks.

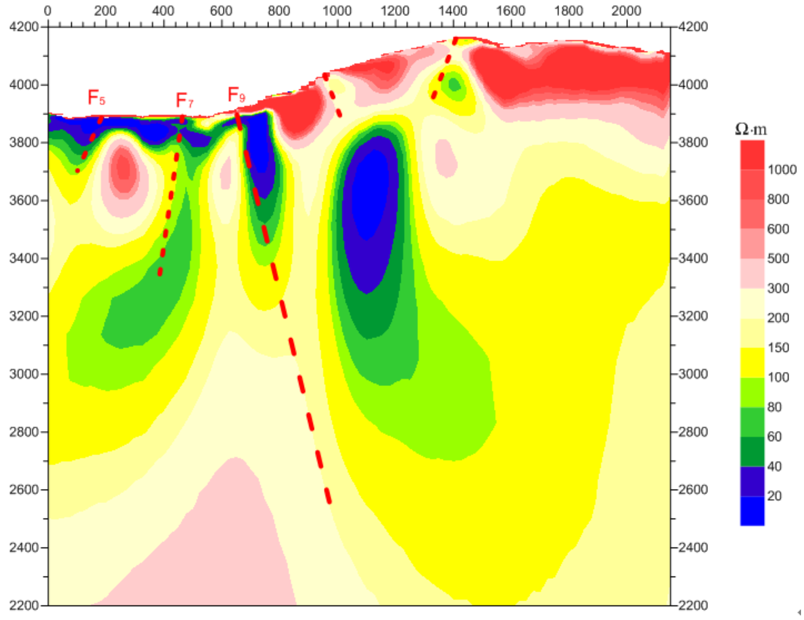

Figure 5: The two-dimensional inversion cross section map of AMT (L2)

(2) L4 AMT section

There is an obvious low resistance anomaly area under the range of 650–760 m of the section L4, interpreted to be the E-dipping fault F7, with a dip angle of 76° (Fig.6). Compared with the fault F7 shown in the section L2, the dip angle has been changed. In addition, low resistance anomaly areas were identified under the ranges of 840–880 m and ca. 1800 m of the section L4, and they were interpreted as the faults F9 and F4, respectively. The fault F9 is an E-dipping fault with a dip angle of 74°, while F4 is a W-dipping fault. Similar to the section L2, the low resistance anomaly channel connects the F7 and F9 with each other in the section L4; while a difference is that the depth of low resistance anomaly area in section L4 is much shallower than that in L2. The low resistance anomaly area in section L4 is < 40 m in the depth, and ca. 20 m in the thickness. It is interfered the Quaternary is 80 m in the thickness based on the low resistance anomaly under the range of 80–760 m. Compared with the eastern part of the section, a relative high resistance body (< 40 m in the thickness) exists under the range of 80–400 m in the western part of the section, which is regarded as Quaternary Alluvial and diluvial deposits.

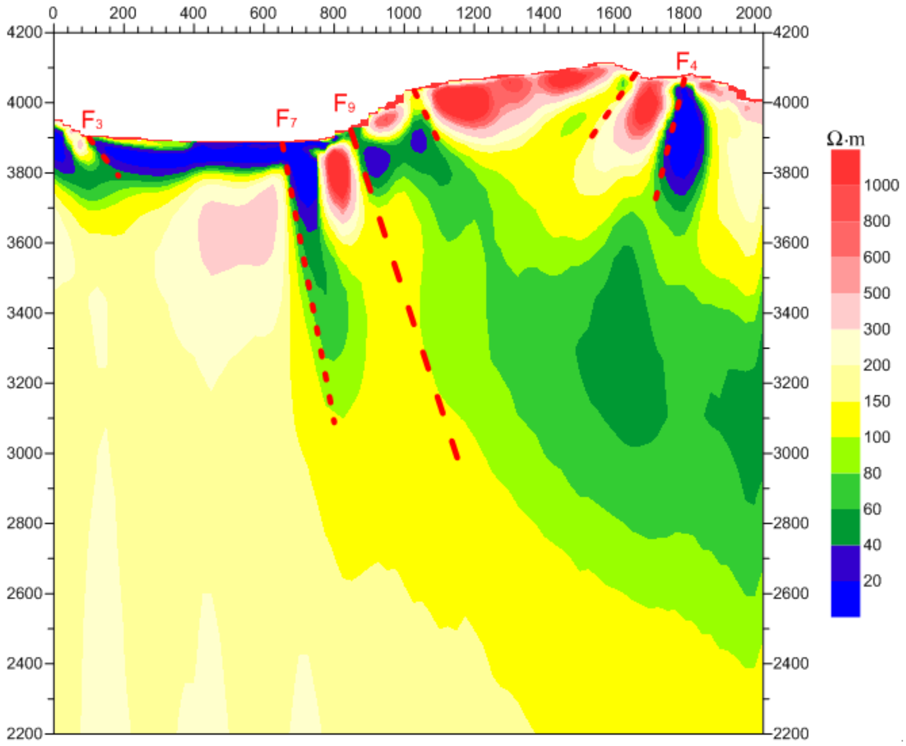

Figure 6: The two-dimensional inversion cross section map of AMT (L4)

5. GEOTHERMAL RESERVOIR MODEL

A geothermal reservoir model of the Xumai geothermal field was established based on the geological, hydrological, geophysical and geochemical works (Fig. 7). In this model, the F1 and its secondary fractures play an important role in controlling the geothermal reservoir in the deep. The locations of shallow and deep geothermal reservoirs and the cyclic process of surface and underground water were marked in the model. Two types of thermal reservoirs exists in the prospective area of the Xumai village, one is shallow stratified reservoir with a depth of 0–200 m and the other is zoned reservoir in base rocks with a depth of 200–1000 m. The zoned reservoir in base rocks was control by the fault F1 and its secondary fractures F5, F7 and F9. The deep underground hot water is supplied from the mountains in the eastern, northern and western of the basin along the NS-striking deep-large faults.

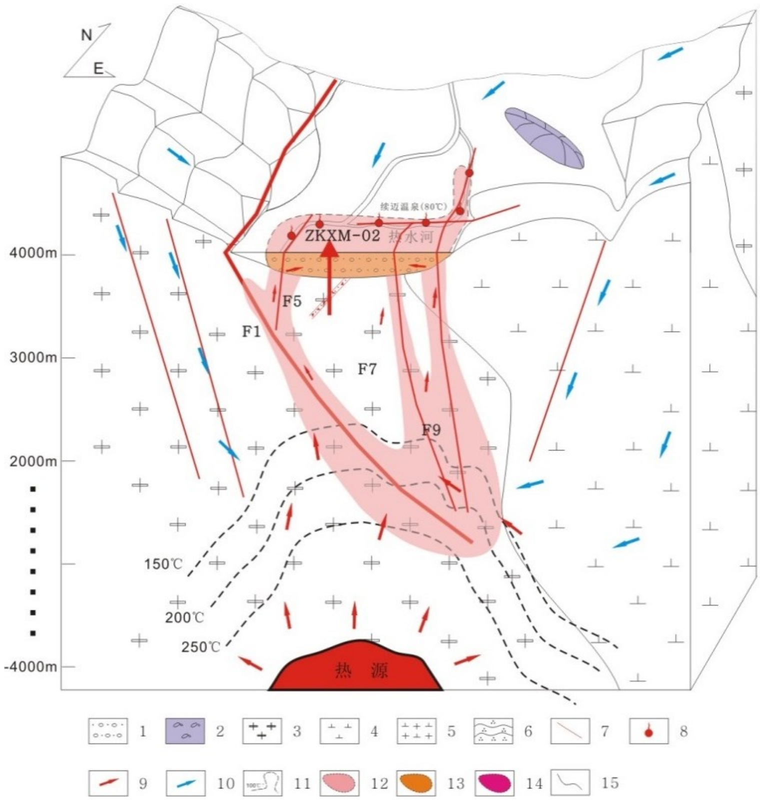

Figure 7: The geothermal reservoir model of the Xumai geothermal field

1-quaternary; 2-glacial drift; 3-porphyritic monzonitic granite; 4-diorite; 5-granodiorite; 6-slate; 7-fault; 8-hot spring; 9-hot water migration; 10- cold water migration; 11-inferred isotherm; 12-geothermal anomalies of the surface; 13-hot water in the quaternary; 14- hot water in the batholith; 15-the boundary of the rock

6. CONCLUSIONS

The distribution of the geothermal anomaly areas are along the fault F1 and its secondary structures; the clay-alternation relating to the geothermal activities also distribute along the F1, and the remains of the ancient sinter were also observed here. The geothermal reservoir of the Xumai Basin was controlled by the F1 and its secondary structures.

The supplies of the underground water are mainly from the atmospheric precipitation (river) on the both sides of the basin, and partly come from the river in the northern. Groundwater discharge forms are mainly springs, artificial drillings, and evaporation. The chemical type of surface water and cold spring water in the work area is HCO_3-Ca. The chemical types of the hot spring water is SO_4·Cl-Na of the Xumai spring , and that is Cl·HCO_3·SO_4-Na of the Angang spring. According to the hydrochemical conditions, higher geothermal fluid may exist under the Angang geothermal anomaly area.

A geothermal reservoir model of the Xumai geothermal field has been established. We considered that the Xumai village geothermal anomaly area is a good target for the drilling, because of its shallow thermal reservoir, massive water and proper temperature. The thermal fluid with higher temperature maybe found in the Angang village and Jiba village geothermal anomaly area.

REFERENCES

Duo, J.: The Basic Characteristics of the Yangbajing Geothermal field, a Typical High Temperature Geothermal System, *Eng. Sci.* **1**, (2003), 42-47 (in Chinese with English abstract).

Liu, Z., Lin, W.J., Zhang, M., Xie, E.J., Liu, Z.M., and Wang, G.L.: Geothermal Fluid Fenesis and Mantle Fluids Contributions in Nimu–Naqu. Tibet. *Earth Sci. Front.*, **21**, (2014), 356-371 (in Chinese with English abstract).

Zhao, P., Jin, J., Zhang, H.Z., Duo, J., and Liang, T.: Chemical Composition of Thermal Water in the Yangbajing Geothermal Field, Tibet. *Scientia Geologica Sinica*, **33**, (1998), 61-72 (in Chinese with English abstract).

Zhao, P., Xie, E.J., Duo, J., Jin, J., Hu, X.C., Du, S.P., and Yao, Z.H.: Geochemical Characteristics of Geothermal Gases and Their Geological Implications in Tibet. *Acta Petrologica Sinica*, **18**, (2002.), 539–550 (in Chinese with English abstract).

Pang, Z.H., and Reed, M.: Theoretical Chemical Thermometry on Geothermal waters: Problems and Methods. Geochim. *Cosmochim. Acta*, **62**, (1998), 1083-1091.

Yuan, J.F., Guo, Q.H., and Wang, Y.X.: Geochemical Behaviors of Boron and Its Isotopes in Aqueous Environment of the Yangbajing and Yangyi Geothermal Fields, Tibet, China, *Geochem. Explor.*, **140**, (2014), 11-22.

Guo, Q.H., Wang, Y.X., Liu, W.: Major Hydrogeochemical Processes in the Two Reservoirs of the Yangbajing Geothermal Field, Tibet, China. J. *Volcanol. Geotherm. Res.*, **166**, (2007), 255-268.

Wang, X., Wang, G.L., Lu, C., Gan, H.N., and Liu, Z.: Evolution of Deep Parent Fluids of Geothermal Fields in the Nimu–Nagchu Geothermal Belt, Tibet, China, *Geothermics*, **71**, (2018), 118-131.